

# Quantifying the Joint Distribution of Drought Indicators in Borneo Fire-Prone Area

M K Najib<sup>1\*</sup>, S Nurdianti<sup>1</sup> and A Sopaheluwakan<sup>2</sup>

<sup>1</sup> Department of Mathematics, Faculty of Mathematics and Natural Science, IPB University, Bogor 16680, Indonesia

<sup>2</sup> Center for Applied Climate Services, Agency for Meteorology, Climatology, and Geophysics, Jakarta 10720, Indonesia

\*Corresponding e-mail: mkhoirun\_najib@apps.ipb.ac.id

**Abstract.** Borneo island is prone to fire due to its large peat soil area. Fire activity in Borneo is associated with regional climate conditions, such as total precipitation, precipitation anomaly, and dry spells. Thus, knowing the relationship between drought indicators can provide preliminary knowledge in developing a fire risk model. Therefore, this study aims to quantify the copula-based joint distribution and to analyze the coincidence probability between drought indicators in Borneo fire-prone areas. From dependence analysis, we found that the average of 2 months of total precipitation (TP), monthly precipitation anomalies (PA), and the total of 3 months of dry spells (DS) provides a moderate correlation to hotspots in Borneo. The results show the probability of the dry-dry period is 26.83, 17.86, and 18.54% for TP-DS, PA-DS, and TP-PA, respectively. All of these are higher than the probability of the wet-wet period, which is 24.41, 16.30, and 17.98% for TP-DS, PA-DS, and TP-PA, respectively. Through the probability, the return period of TP-DS in the dry-dry situation is 44.72 months or 3.7 years, meaning the dry conditions in total precipitation and dry spells that occur simultaneously could appear once every 3.7 years on average. Furthermore, the return period of PA-DS and TP-PA in the dry-dry situation is 5.6 years and 5.4 years, respectively. Moreover, the probability of dry spells in dry condition when given total precipitation in dry condition is higher than given precipitation anomalies in dry condition.

**Keywords:** Coincidence Probability, Copula, Drought, Dry Spells, Precipitation

**Track Name:** Atmospheric Chemistry and Physics

## 1. Introduction

Borneo island is prone to fire due to its large peat soil area, especially in Central Kalimantan Province, Indonesia [1]. In 2015, this province contained 30,400 km<sup>2</sup> peatland and experienced very high numbers of peatland hotspots which is 20,300 hotspots [2]. The conversion of peat forests to agricultural land has further exacerbated the problem by substantially increasing fuel loads and associated fire risk [3,4]. Fire activity in Borneo are sensitive to local climate conditions, such as total precipitation, precipitation anomaly, and dry spells (i.e., precipitation less than 1 mm/day) [5] and regional climate conditions such as El Nino-Southern Oscillation (ENSO). Madadgar et al (2021) define the fire risk model as the conditional probability of fire size given a specific climate condition

[6]. Therefore, knowing the relationship between drought indicators is important as preliminary knowledge in developing a fire risk model.

The copula-based joint distribution can be employed to determine the relationship between the drought indicators. From the joint distribution, coincidence probability analysis [7] can investigate the frequency of the combination of two drought indicator periods, such as the frequency of dry-dry or wet-wet periods. Coincidence probability usually uses in hydrological frequency analysis [8,9]. However, very few experts use this coincidence probability analysis to identify coincidence between drought indicators conditions.

From the description above, this study aims to quantify the copula-based joint distribution and to analyze the coincidence probability between drought indicators in Borneo fire-prone areas. The study results can build knowledge about the relationship between drought indicators and become preliminary knowledge in developing a fire risk model in the future.

## 2. Materials and Methodology

### 2.1 Study area and data

The area in this study is limited to Borneo fire-prone areas selected based on clustering using the unsupervised learning method, which is a k-means algorithm [10]. The clustering uses hotspot data obtained from the National Institute of Aeronautics and Space of Indonesia (LAPAN). The data derived from the Moderate Resolution Imaging Spectroradiometer (MODIS) sensors of the Terra and Aqua Satellites with a spatial resolution of  $0.25^\circ \times 0.25^\circ$  from 2001-2020. We only use hotspot data with a confidence level of more than 80% [5,11]. After defining the fire-prone area in Borneo, drought indicators such as total precipitation, precipitation anomalies, and dry spell processed using converted precipitation data based on a satellite-derived product of SEMDP (The Space-based Weather and Climate Extremes Monitoring Demonstration Project). We use precipitation data based on Climate Prediction Center Morphing Technique (CMORPH) corrected for bias, known as CMORPH bias-corrected product (CMORPH CRT) [12]. The monthly total precipitation and precipitation anomaly data were processed using the CMORPH CRT monthly data. Meanwhile, the monthly dry spell data was processed using the CMORPH CRT daily data.

### 2.2 Dependence analysis

Kendall's rank correlation  $\tau$  measures the degree of association between variables to capture any non-linear relationships, then  $\tau$  has several desired properties over other rank correlation measures [13]. Each of the variables pair determines the statistically significant correlation [14].

Extremal dependence falls into two classes: asymptotic dependence or asymptotic independence [15]. Let  $(X,Y)$  is a pair of variables with distribution functions  $(F_X, F_Y)$ ,  $\chi$  is the extremal dependence of  $(X,Y)$  [16]. Using transformed uniform(0,1) distributions, i.e.  $U = F_X(X)$ ,  $V = F_Y(Y)$ , the coefficient  $\chi$  is given by

$$\chi(u) = 2 - \frac{\ln[P(U < u, V < v)]}{\ln[P(U < u)]} \quad (1)$$

where  $\chi = \lim_{u \rightarrow 1} \chi(u)$  for  $0 \leq u \leq 1$  and  $0 \leq \chi \leq 1$ . If  $\chi = 0$  and  $\chi = 1$ , the variable pair fall into asymptotically independent and perfect dependence, respectively. In the case of asymptotic independence ( $\chi = 0$ ), the measure  $\bar{\chi}$  uses to quantify the magnitude of the dependence of asymptotically independent variables

$$\bar{\chi} = \frac{2\ln[P(U > u)]}{\ln[P(U > u, V > u)]} - 1 \quad (2)$$

where  $\bar{\chi} = \lim_{u \rightarrow 1} \bar{\chi}(u)$  for  $-1 \leq \bar{\chi} \leq 1$ . For positive association variables  $\bar{\chi} = 1$ , for negative association variables  $\bar{\chi} = -1$ , and nearly independent variables  $\bar{\chi} = 0$  [14,16,17].

### 2.3 Copulas

For bivariate copula, let a 2-dimensional random vector  $X$  with marginal cumulative distribution function  $F_{X_1}$  and  $F_{X_2}$  in  $\mathbb{R}$ , i.e., non-decreasing,  $F_{X_1}(-\infty)=0$  and  $F_{X_1}(\infty)=1$ . Sklar's theorem [18] says that the joint distribution  $F_X$  of this random vector is a function of its marginal distributions

$$F_X(x_1, x_2) = C(u_1, u_2) \quad (3)$$

where  $C_X : [0,1] \times [0,1] \rightarrow [0,1]$  is a joint distribution function of the transformed random variables  $u_i = F_{X_i}(x_i) \sim \text{uniform}(0,1)$  for  $i=1,2$  [19,20]. We assume continuous and differentiable distribution functions  $F_{X_1}$  and  $F_{X_2}$ . Thus,  $C_X$  is unique and can be expressed by

$$C_X(u_1, u_2) = \int_0^{u_1} \int_0^{u_2} c_X(u'_1, u'_2) du'_2 du'_1 \quad (4)$$

where  $u_i = F_{X_i}(x_i)$  for  $i=1,2$ . The function  $C_X$  is a copula function, while  $c_X$  is the corresponding copula density function. The important consequence of Sklar's theorem is that every joint probability density is also writable by the product of the marginal probability densities and the copula density.

$$f_X(x_1, x_2) = f_{X_1} \cdot f_{X_2} \cdot c_X(u_1, u_2) \quad (5)$$

There are many types of copula functions [7]. Different copulas differ in describing the dependence structures [21]. Eleven bivariate copulas are selected, including one-parameter and two-parameter copulas given in Table 1 [19,21–28].

**Table 1.** The cumulative density functions and parameter ranges of selected bivariate copulas.

No	Copula	$C_X(u_1, u_2)$	Parameter Range
1	Normal	$F_{N(0,\Sigma)}(F_{N(0,1)}^{-1}(u_1), F_{N(0,1)}^{-1}(u_2))$	
2	Student-t	$F_{t(v,\Sigma)}(F_{t(v)}^{-1}(u_1), F_{t(v)}^{-1}(u_2))$	
3	Clayton	$(u_1^{-\theta} + u_2^{-\theta} - 1)^{-1/\theta}$	$\theta > 0$
4	Gumbel	$\exp[-(w_1^\theta + w_2^\theta)^{1/\theta}]$ , where $w_i = -\ln(u_i)$	$\theta \geq 1$
5	Frank	$-\frac{1}{\theta} \ln \left[ 1 + \frac{w_1 w_2}{(e^{-1} - 1)} \right]$ , where $w_i = e^{-\theta u_i} - 1$	$\theta \neq 0$
6	Joe	$1 - (1 - w_1 w_2)^{1/\theta}$ , where $w_i = 1 - (1 - u_i)^\theta$	$\theta \geq 1$
7	Galambos	$u_1 u_2 \exp[(w_1^{-\theta} + w_2^{-\theta})^{-1/\theta}]$ , where $w_i = -\ln(u_i)$	$\theta \geq 0$
8	BB1	$[1 + (w_1^\delta + w_2^\delta)^{1/\delta}]^{-1/\theta}$ , where $w_i = u_i^{-\theta} - 1$	$\theta > 0, \delta \geq 1$
9	BB6	$1 - \{1 - \exp[-(w_1^\delta + w_2^\delta)^{1/\delta}]\}^{1/\theta}$ , where $w_i = -\ln[1 - (1 - u_i)^\theta]$	$\theta \geq 1, \delta \geq 1$
10	BB7	$1 - [1 - (w_1^{-\delta} + w_2^{-\delta} - 1)^{-1/\delta}]^{1/\theta}$ , where $w_i = 1 - (1 - u_i)^\theta$	$\theta \geq 1, \delta > 0$
11	BB8	$\frac{1}{\theta} \left\{ 1 - \left[ 1 - \frac{w_1 w_2}{1 - (1 - \delta)^\theta} \right]^{1/\delta} \right\}$ , where $w_i = 1 - (1 - \delta u_i)^\theta$	$\theta \geq 1, 0 < \delta \leq 1$

**Note.** BB1 (Clayton-Gumbel), BB6 (Joe-Clayton), BB7 (Joe-Gumbel), and BB8 (Joe-Frank). Normal and student-t employ the linear correlation  $\rho$  as a parameter.

### 2.4 Copula parameter estimation and goodness of fit

We use the inference of functions for margins (IFM) method to estimate the parameters of copulas [29]. The IFM method is a 2-step estimation method for the copula parameter  $\theta$ . In the first step, estimate the parameters  $\alpha_j$  (notated  $\hat{\alpha}_j$ ) of each marginal distribution separately using  $X_1, X_2$ . In the second step, approximate the parameter  $\theta$  by replacing  $\alpha_j$  using  $\hat{\alpha}_j$  in the log-likelihood function as

$$\hat{\theta} = \arg \max \sum_{t=1}^n \ln c_X [F_{X_1}(x'_1; \hat{\alpha}_1), F_{X_2}(x'_2; \hat{\alpha}_2); \theta] \quad (6)$$

where  $\hat{\theta}$  is the estimated parameter for  $\theta$  [7,30]. In this study, Kolmogorov–Smirnov error ( $D_n$ ) [7], Root Mean Square Error (RMSE) [26], and Akaike’s information criterion (AIC) [31] measure the goodness of fit of the joint distributions as follows:

$$\text{Kolmogorov-Smirnov Error } (D_n): \max_{i=1,2,\dots,n} |P_{Ei} - P_{Ti}| \quad (7)$$

$$\text{Root Mean Square Error (RMSE): } \sqrt{\frac{1}{n} \sum_{i=1}^n (P_{Ei} - P_{Ti})^2} \quad (8)$$

$$\text{Akaike’s information criterion (AIC): } 2k - 2\ln L \quad (9)$$

where  $n$  is the sample size,  $k$  is the number of parameters of different distributions,  $L$  is the maximum likelihood function value of distributions,  $P_{Ei}$  and  $P_{Ti}$  are the empirical and theoretical frequency, respectively. Assuming the variables  $X$  and  $Y$  with the same length, Gringorten’s formula can estimate the frequency of bivariate variables  $X$  and  $Y$  as follow

$$P_{Ei} = P(X \leq x_i, Y \leq y_i) = \frac{\#(X \leq x_i, Y \leq y_i) - 0.44}{n + 0.12} \quad (10)$$

where  $(x_i, y_i)$  is the combination of the  $i$ -th values of the increased order in the  $X$  and  $Y$  series.

### 2.5 Coincidence probability

The drought coincidence probability represents the frequency  $P$  in wetness, dryness, or normal condition, while the other indicator is wetness, dryness, or normal condition. To distinguish dry, normal, and wet conditions, tercile categories (i.e., below-normal, near-normal, and above-normal) are usually used [32]. Thus, this study uses the 1/3 and 2/3 quantiles as thresholds to define the condition of wetness and dryness in drought indicators conditions. As mentioned above, drought indicators include total precipitation, precipitation anomalies, and dry spells. For suitability, we used negative of total precipitation and negative of precipitation anomalies. Thus, for the drought indicator  $X$ ,  $X_w$  and  $X_d$  were assigned the threshold quantiles of wetness ( $P_w = 1/3$ ) and dryness ( $P_d = 2/3$ ), respectively. Therefore, the degree of the wet-dry conditions is represented as wetness ( $X < X_w$ ), dryness ( $X \geq X_d$ ), and normalness ( $X_w \leq X < X_d$ ). Thus, the wet-wet and dry-dry periods are given by

$$\begin{aligned} P_{ww} &= P(X < X_w, Y < Y_w) = C_X(u_w, v_w) \\ P_{dd} &= P(X \geq X_d, Y \geq Y_d) = 1 - u_d - v_d + C_X(u_d, v_d) \end{aligned} \quad (11)$$

where  $u$  and  $v$  are the marginal distribution of  $X$  and  $Y$ , while subscripts  $w$ ,  $n$ , and  $d$  indicate wetness, normal, and dryness. For example,  $dd$  presents the dry–dry condition, and  $P_{dd}$  is the coincidence probability of this condition [7].

## 3. Results and Discussion

### 3.1 Identification of the Borneo fire-prone area using unsupervised learning

The unsupervised learning method, i.e., k-means clustering, mentioned above was used to identify the fire-prone areas in Borneo. K-means algorithm is a simple iteration method to partition a given dataset into  $k$  numbers of user-defined clusters [33]. This study selects 8-means clusters, and Figure 1 shows the results of the clustering process.

Figure 1(a) shows the entire cluster area using the k-means clustering. Each color represents a different cluster. For example, cluster 1 (dark blue) is an area with a few hotspot characteristics [5]. From 969 grid points in Borneo, cluster 1 covers 679 grid points, about 70% of Borneo Island, i.e., Malaysia, Brunei, and most East and North Kalimantan Provinces. In cluster 1, the maximum hotspot occurrence is only about 3.43 hotspots per grid point data on average, i.e., in 2002. Thus, we assume that cluster 1 is a low fire-prone area and removed from the study area, and the result area is given in Figure 1(c). After removing cluster 1 from the study area, the total monthly hotspots decreased slightly compared to the entire cluster but did not change the pattern, as seen in Figures 1(b) and 1(d).

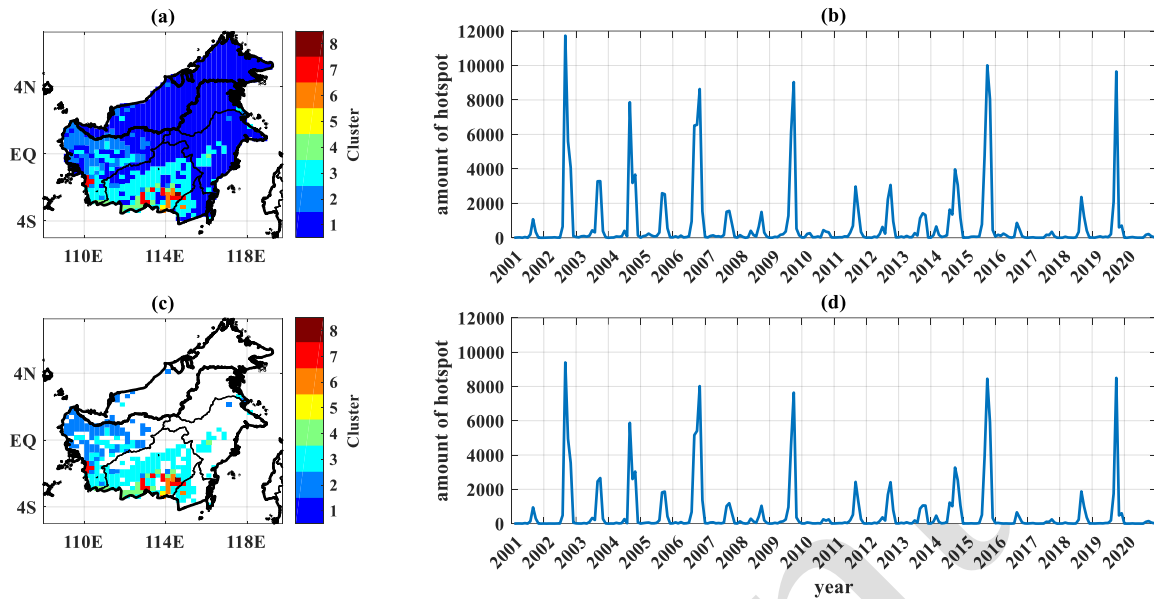


**Figure 1.** Clustering result of hotspots in Borneo in 2001-2020 using k-means clustering: (a) areas with all clusters, (b) total monthly hotspots of all clusters, (c) areas without cluster 1, and (d) total monthly hotspots without cluster 1.

### 3.2 Dependence analysis between drought indicators and total hotspot

After identifying the fire-prone areas, CMORPH precipitation data extracted to derive the drought indicators in the Borneo fire-prone area from 2001-2020. After that, each data grid point aggregated on average. Thus, the time-series data represent the aggregate of drought conditions in Borneo fire-prone areas. Kendall and extremal dependencies mentioned above are employed to identify the association of each drought indicator to the total hotspots at several lag times, as seen in Table 2.

**Table 2.** Assessment of the association between drought indicators and total hotspot.

Lag	Neg TP – Hotspots			Neg PA – Hotspots			DS – Hotspots		
	$\tau$	$\chi$	$\bar{\chi}$	$\tau$	$\chi$	$\bar{\chi}$	$\tau$	$\chi$	$\bar{\chi}$
0	<b>0.463</b>	<b>0.441</b>	<b>0.481</b>	<b>0.265</b>	<b>0.428</b>	<b>0.473</b>	<b>0.473</b>	<b>0.514</b>	<b>0.534</b>
1	<b>0.453</b>	<b>0.469</b>	<b>0.530</b>	0.163	0.186	0.164	<b>0.444</b>	<b>0.555</b>	<b>0.598</b>
2	0.346	0.397	0.406	0.132	0.213	0.125	<b>0.321</b>	<b>0.421</b>	<b>0.439</b>
3	0.182	0.230	0.127	0.045	0.195	0.030	0.139	0.215	0.107

Total precipitation and dry spells had moderate associations with hotspots ( $\tau \geq 0.3$ ) at a time lag of 0 to 2 months and statistically significant correlations at a time lag of 3 months, although the correlation was small. In contrast, precipitation anomalies had a small association with hotspots ( $\tau < 0.3$ ) but statistically significant correlations at a time lag of 0 to 2 months. Besides, the peaks in the correlations are zero lag at all drought indicators, representing that hotspot occurrence in fire-prone areas in Borneo is most influenced by drought indicators in the same month.

To ensure the association of drought indicators, especially at the extreme, Extremal dependencies are employed. Despite having a small Kendall- $\tau$  correlation, precipitation anomalies have a moderate positive association at extreme values at zero lag ( $\chi > 0.4$ ). Meanwhile, dry spells have Extremal dependencies on lags 0, 1, and 2. A confusing thing occurs in total precipitation, where Extremal dependency on lag 2 is not high enough but has a moderate correlation. For differing with dry spells, this study assumes that total precipitation only has Extremal dependencies up to lag 1. Moreover, at lag 3, drought indicators nearly independent at the extreme ( $\bar{\chi} \rightarrow 0$ ). Consequently, the drought indicators we will use in this study are the average of 2 months total precipitation, monthly precipitation anomalies, and the total of 3 months of dry spells.

### 3.3 Copula parameter estimation and goodness of fit

As mentioned above, we use the inference of functions for the margins (IFM) method to estimate the copula parameter. We use generalized extreme value and lognormal distributions to identify the univariate marginal distribution of drought indicators [7,34]. Also, we use the Anderson-Darling test to test the feasibility of fitting these distributions to the data. A-D test returns a test decision for the null hypothesis that the data is from a population with a defined distribution. Table 3 shows the result of the marginal distribution fitting process.

**Table 3.** The result of the marginal distribution fitting process using generalized extreme value and lognormal distribution.

	Neg of Total Precipitation	Neg of Precipitation Anomaly	Dry Spells
Distribution	Generalized Extreme Value	Generalized Extreme Value	Lognormal
A-D Test (p-value)	Do not reject (0.3474)	Do not reject (0.9732)	Do not reject (0.0598)

*Note.* Do not reject based on a 5% significance level.

The statistical result shows that the chosen distribution all passed the Anderson-Darling test with a 5% significance level. The negative of the total precipitation and precipitation anomalies are fit using generalized extreme value distribution, while the dry spell is more fit using lognormal distribution. The second step of the IFM method is estimating the copula parameter, as seen in Equation (6). Eleven selected bivariate copulas in Table 1 are constructed, and their parameters are estimated. Table 4 shows that BB6, Gumbel, and BB7 copulas are the fittest model for bivariate joint distribution between Total Precipitation-Dry Spells (TP-DS), Precipitation Anomalies-Dry Spells (PA-DS), and Total Precipitation-Precipitation Anomalies (TP-PA), respectively.

**Table 4.** Top three results of the bivariate copula parameter fitting process ordered by Akaike's information criterion (AIC) between TP-DS, PA-DS, and TP-PA.

No	TP-DS		PA-DS		TP-PA	
	Copula	(Dn, RMSE, AIC)	Copula	(Dn, RMSE, AIC)	Copula	(Dn, RMSE, AIC)
1	BB6	(0.1078,0.0380,-343.6)	Gumbel	(0.0802,0.0234,-55.5)	BB7	(0.0567,0.0173,-82.7)
2	Galambos	(0.1061,0.0379,-342.8)	Joe	(0.0798,0.0262,-55.3)	BB1	(0.0557,0.0161,-81.5)
3	Gumbel	(0.1063,0.0380,-342.6)	Galambos	(0.0796,0.0234,-54.6)	Galambos	(0.0572,0.0171,-81.3)

### 3.4 Joint probability density function between drought indicators

The selected bivariate copula between TP-DS, PA-DS, and TP-PA are visualized using a contour plot of the joint probability density function and given in Figure 2. As mentioned in equation 5, the joint probability density function is the product of the marginal probability densities and the copula probability density function. The results show that the joint distribution between TP-DS, PA-DS, and TP-PA has an upper tail dependency. In this case, an upper tail dependency represents that the probability of dry-dry conditions is higher than wet-wet conditions. This is because this study area only covers fire-prone areas in Borneo (but not flood-prone areas) so that extreme wet events are not visualized in the joint distribution.

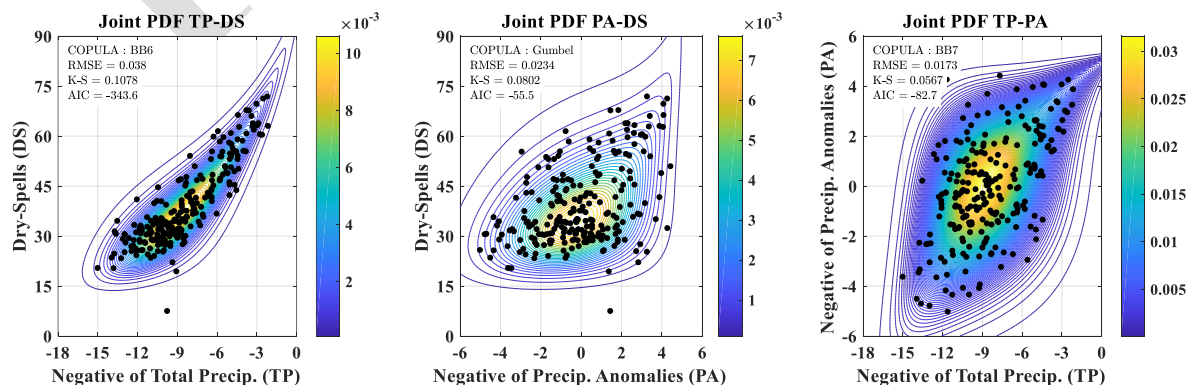


**Figure 2.** Contour plot of the joint probability density function between TP-DS, PA-DS, and TP-PA.

As mentioned above, this study uses the 1/3 and 2/3 quantiles as thresholds to define the condition of wetness and dryness in drought coincidence. Based on the result of the fitting process in Table 3, for wetness condition, we use  $X_w = -9.8306$ ,  $Y_w = -0.9513$ , and  $Z_w = 32.8817$  as a threshold for negative of total precipitation, negative of precipitation anomalies, and dry spells, respectively. Meanwhile, for dryness conditions, we use  $X_d = -7.4105$ ,  $Y_d = 0.9370$ , and  $Z_d = 42.4576$  as a threshold for negative of total precipitation, negative of precipitation anomalies, and dry spells, respectively. Using equation (11), the probability of the dry-dry period ( $P_{dd}$ ) is 26.83, 17.86, and 18.54% for TP-DS, PA-DS, and TP-PA, respectively. All of these are higher than the probability of the wet-wet period ( $P_{ww}$ ), which is 24.41, 16.30, and 17.98% for TP-DS, PA-DS, and TP-PA, respectively, indicating the frequency of co-occurrence in dry conditions between the two drought indicators is higher than in wet conditions.

Through the probability, the return period of TP-DS in the dry-dry situation is 44.72 months or 3.7 years, meaning the dry conditions in total precipitation and dry spells that occur simultaneously could appear once every 3.7 years on average. Furthermore, the return period of PA-DS and TP-PA in the dry-dry situation is 5.6 years and 5.4 years, respectively. From the coincidence probability, the conditional probability of dry spells in the dry situation given specific total precipitation in the dry situation is

$$P_{Z|X}(Z \geq Z_d | X \geq X_d) = \frac{P_{X,Z}(X \geq X_d, Z \geq Z_d)}{P_X(X \geq X_d)} = \frac{26.83\%}{1/3} = 80.49\%$$

and given specific precipitation anomaly in the dry situation is

$$P_{Z|Y}(Z \geq Z_d | Y \geq Y_d) = \frac{P_{X,Y}(X \geq X_d, Y \geq Y_d)}{P_X(X \geq X_d)} = \frac{17.86\%}{1/3} = 53.58\%$$

They implied that if given total precipitation in the dry situation (i.e., less than 7.41 mm/day), the probability of dry spells in the dry situation (i.e., more than 42.5 days) is 80.49%. Otherwise, if given precipitation anomaly in the dry situation (i.e., less than -0.937 mm/day), the probability of dry spells in the dry situation (i.e., more than 42.5 days) is 53.58%.

#### 4. Conclusions

The drought indicator is an important variable that leads to many hotspots in Borneo. Therefore, knowing the relationship between drought indicators can provide preliminary knowledge in developing a fire risk model, which is the conditional probability of hotspots given a specific climate condition (such as drought indicators).

From dependence analysis, we found that the average of 2 months of total precipitation (TP), monthly precipitation anomalies (PA), and the total of 3 months of dry spells (DS) provides a moderate correlation to hotspots in Borneo. Based on these three variables, the bivariate copula was calculated. The results show the probability of the dry-dry period ( $P_{dd}$ ) is 26.83, 17.86, and 18.54% for TP-DS, PA-DS, and TP-PA, respectively. All of these are higher than the probability of the wet-wet period ( $P_{ww}$ ), which is 24.41, 16.30, and 17.98% for TP-DS, PA-DS, and TP-PA, respectively. Through the probability, the return period of TP-DS in the dry-dry situation is 44.72 months or 3.7 years, meaning the dry conditions in total precipitation and dry spells that occur simultaneously could appear once every 3.7 years on average. Furthermore, the return period of PA-DS and TP-PA in the dry-dry situation is 5.6 years and 5.4 years, respectively. Moreover, the probability of dry spells in dry condition when given total precipitation in dry condition is higher than given precipitation anomalies in dry condition.

#### References

- [1] Yulianti N et al. 2020 *ECOTROPHIC J. Ilmu Lingkungan*. **14** (1): 62–73
- [2] Miettinen J, Shi C, and Liew SC 2017 *Environ. Manage.* **60** (4): 747–57

- [3] Wijedasa LS et al. 2017 *Glob. Chang. Biol.* **23** (3): 977–82
- [4] Santika T et al. 2020 *Glob. Environ. Chang.* **64**: 102129
- [5] Nurdianti S, Sopaheluwakan A, and Septiawan P 2021 *Agromet.* **35** (1): 1–10
- [6] Madadgar S et al. 2020 *Stoch. Environ. Res. Risk Assess.* **34** (12): 2023–31
- [7] Wei X et al. 2020 *Hydrol. Res.* **51** (5): 1120–35
- [8] Yan B and Chen L 2013 *J. Hydrol.* **499**: 19–26
- [9] Du H, Wang Y, Liu K, and Cheng L 2019 *Environ. Earth Sci.* **78** (7): 1–12
- [10] Khairani NA and Sutoyo E 2020 *Int. J. Adv. Data Inf. Syst.* **1** (1): 9–16
- [11] Ardiansyah M, Boer R, and Situmorang AP 2017 *IOP Conf. Ser. Earth Environ. Sci.* **54** (1): 012058
- [12] Sun R, Yuan H, Liu X, and Jiang X 2016 *J. Hydrol.* **536**: 302–19
- [13] Li G, Peng H, Zhang J, and Zhu L 2012 *Ann. Stat.* **40** (3): 1846–77
- [14] Jane R, Cadavid L, Obeysekera J, and Wahl T 2020 *Nat. Hazards Earth Syst. Sci.*: 1–30
- [15] Ledford AW and Tawn JA 1997 *J. R. Stat. Soc. Ser. B Stat. Methodol.* **59** (2): 475–99
- [16] Coles S, Heffernan J, and Tawn J 1999 *Extrem.* **2** (4): 339–65
- [17] Tilloy A, Malamud B, Winter H, and Joly-Laugel A 2020 *Nat. Hazards Earth Syst. Sci.* **20** (8): 2091–117
- [18] Sklar M 1959 *Publ. L'Institut Stat. L'Université Paris.* **8**: 229–31
- [19] Schölzel C and Friederichs P 2008 *Nonlinear Process. Geophys.* **15** (5): 761–72
- [20] Laux P et al. 2011 *Hydrol. Earth Syst. Sci.* **15** (7): 2401–19
- [21] Li Z, Shao Q, Tian Q, and Zhang L 2020 *Hydrol. Res.* **51** (5): 867–81
- [22] Bezak N, Mikoš M, and Šraj M 2014 *Water Resour. Manag.* **28** (8): 2195–212
- [23] Orcel O, Sergeant P, and Ropert F 2020 *Nat. Hazards Earth Syst. Sci.* **21** (1): 239–60
- [24] de Melo Mendes B and de Souza R 2004 *Int. Rev. Financ. Anal.* **13** (1): 27–45
- [25] Zhang L and Singh VP 2007 *J. Hydrol. Eng.* **12** (4): 409–19
- [26] Zhang L and Singh VP 2019 *Symmetric Archimedean Copulas In Copulas and their Applications in Water Resources Engineering* (Cambridge University Press) chapter 4 pp 123–71
- [27] Aldhufairi FAA, Samanthi RGM, and Sepanski JH 2020 *Risks.* **8** (4): 106
- [28] Buike A 2018 *Copula Modeling for World's Biggest Competitors* (Ph.D. Dissertation, Universiteit van Amsterdam)
- [29] Joe H 2005 *J. Multivar. Anal.* **94** (2): 401–19
- [30] Bouyé E et al. 2000 *Copulas for Finance - A Reading Guide and Some Applications* (<https://dx.doi.org/10.2139/ssrn.1032533>)
- [31] Tahroudi MN, Ramezani Y, De Michele C, and Mirabbasi R 2020 *Hydrol. Res.* **51** (6): 1332–48
- [32] de Andrade FM et al. 2021 *Weather Forecast.* **36** (1): 265–84
- [33] Wu X et al. 2008 *Knowl. Inf. Syst.* **14** (1): 1–37
- [34] Rinaldi A 2019 *Pros. Semin. Nas. Mat. dan Pendidik. Mat.* **2**: 21–38

## Acknowledgments

The authors would like to thank the Department of Mathematics, IPB University, and the Meteorological, Climatological, and Geophysical Agency of Indonesia for their support throughout this research.